

# Transport properties of $\text{Bi}_2\text{Sr}_2\text{CaCu}_2\text{O}_8$ crystals with and without surface barriers

D. T. Fuchs<sup>1</sup>, R. A. Doyle<sup>2</sup>, E. Zeldov<sup>1</sup>, S. F. W. R. Rycroft<sup>2</sup>, T. Tamegai<sup>3</sup>, S. Ooi<sup>3</sup>, M. L. Rappaport<sup>4</sup>, and Y. Myasoedov<sup>1</sup>

<sup>1</sup>*Department of Condensed Matter Physics, The Weizmann Institute of Science, Rehovot 76100, Israel*

<sup>2</sup>*Interdisciplinary Research Center in Superconductivity, University of Cambridge, Cambridge CB3 0HE, England*

<sup>3</sup>*Department of Applied Physics, The University of Tokyo, Hongo, Bunkyo-ku, Tokyo, 113, Japan*

<sup>4</sup>*Physics Services, The Weizmann Institute of Science, Rehovot 76100, Israel*

(July 1, 1998)

$\text{Bi}_2\text{Sr}_2\text{CaCu}_2\text{O}_8$  crystals with electrical contacts positioned far from the edges are studied by transport measurements, then cut into narrow strip geometry, and remeasured. Instead of showing larger resistance, the strips display a dramatic drop in the resistance, enhanced activation energy, and nonlinear behavior due to strong surface barriers. The surface barriers also dominate the resistive drop at the first-order phase transition. Because the surface barriers are avoided in large crystals, we are able to probe the solid phase and find good agreement with the recent predictions of Bragg glass theory.

PACS numbers: 74.25.Dw, 74.25.Fy, 74.60.Ge, 74.72.Hs.

The resistive behavior of high-temperature superconductors (HTSC) is of central importance for both fundamental and applied research. In particular, the transport properties of single crystals of HTSC have been intensively studied to derive valuable information on critical currents, vortex pinning, dissipation mechanisms, I-V characteristics, phase transitions, etc. [1]. These studies are mainly aimed at resolving various aspects of vortex dynamics in the bulk of the superconductors. The samples are usually chosen or cut to be in a long and narrow strip geometry for four probe transport measurements. Longer samples improve the measurement sensitivity, whereas narrower width is usually assumed to ensure a uniform current flow and the ability to achieve higher current densities. In this Letter we demonstrate that this classical geometry turns out to be undesirable for determining the bulk resistive properties, and may result in apparent resistivities which are orders of magnitude lower than the true bulk resistivity.

The current distribution across  $\text{Bi}_2\text{Sr}_2\text{CaCu}_2\text{O}_8$  (BSCCO) crystals has been recently analyzed by measuring the self-induced magnetic field of the transport current [2,3]. It was found that over a wide range of temperatures and fields the transport current flows predominantly at the sample edges [2,3], where vortices enter and exit the crystal, due to the presence of surface barriers (SB) [4–7]. This finding implies that transport measurements may result in a highly erroneous evaluation of the bulk resistivity. The self-field technique, however, does not measure the value of the resistivity and cannot provide quantitative information on the extent of the error. For that purpose the resistivity has to be measured directly with and without the presence of SB. We have therefore devised the following experiment. Four electrical contacts were deposited in the central part of large square-shaped BSCCO crystals, as shown schematically in the inset to Fig. 1, and transport measurements were

carried out in this ‘unconventional’ geometry. Then the crystals were cut along the marked ‘cut lines’ in Fig. 1 to form the ‘standard’ narrow strip geometry, and remeasured.

The described findings were confirmed on several high quality BSCCO single crystals ( $T_c \simeq 89$  K). Here we present results for two of the crystals, grown by the traveling solvent floating zone method [8]. Crystal A was cleaved and cut to dimensions of 1.2 mm ( $w$ ) $\times$ 1.1 mm ( $l$ ) in the  $ab$  plane and 13 $\mu\text{m}$  thick, and was subsequently cut to a 0.36 mm wide strip. Crystal B was initially 1.3 ( $w$ ) $\times$ 1.7 ( $l$ )  $\times$ 0.013 ( $d$ ) mm<sup>3</sup>, and was later cut to 0.29 mm width. Four Ag/Au pads for electrical contacts were thermally evaporated and had dimensions of 100  $\times$  200 $\mu\text{m}^2$  with 75 $\mu\text{m}$  separation. The same contacts were used for transport measurements in the ‘square’ and ‘strip’ geometries. The magnetic field was applied parallel to the crystalline  $c$ -axis, and the four-probe resistance was measured using an ac bridge.

Cutting the crystals is expected to increase their resistance because the cross section is reduced. This is indeed the case at temperatures above  $T_c$  where the resistance of the strip crystals is typically a factor of three larger than before cutting, consistent with the change in the geometry. In contrast, at lower temperatures the cutting *decreases* the measured resistance dramatically, by as much as two orders of magnitude, as shown in Fig. 1 for various fields and temperatures. If the sample resistance is governed by bulk properties, any reduction of the cross section must necessarily lead to an increase of the measured resistance, in striking contrast to the experimental result. The observed large decrease of the resistance of the strip crystals is a direct manifestation of the dominant role of the SB.

In the standard strip geometry in perpendicular field the flowing vortices enter the sample from one edge, flow across the bulk, and exit at the other edge. This pro-

cess involves vortex activation over the SB and drift of vortices across the bulk. Electrically this situation can be represented by parallel resistors,  $R_S$  of the edges and  $R_B$  of the bulk [6]. A large SB impedes vortex transmission through the edges and is equivalent to a low  $R_S$ , which shunts the relatively large bulk  $R_B$ . As a result, the measured sample resistance  $R_S || R_B$  is reduced, and most of the current flows along the low resistance edges of the sample as was demonstrated by the self-field measurements [2,3]. In order to measure the true bulk transport properties one has to use a configuration in which vortices circulate in the bulk without crossing the edges. This situation is approached here by simply using the large square crystals. Since the current contacts are positioned far from all the edges, most of the vortices circulate around the two current contacts, and the measured voltage drop between the voltage contacts is thus determined by bulk vortex properties. Even if the SB is extremely large, so that  $R_S$  vanishes along the entire circumference, the measured resistance is reduced only slightly as compared to an infinite sample with no edges. This is because the distance between the two current contacts is comparable or smaller than their distance from the edges. Hence any current path that includes a segment along the low resistance edges also includes the high resistance segments from the injection contact to the edge and back from the edge to the drain contact. In the strip crystals, on the other hand, the contacts are in close proximity to the edges and thus most of the current is readily shunted by the low resistance edges. Our numerical calculations of current distributions confirm this description and show that the measured resistance of the square crystal reflects mainly the bulk resistance, whereas the resistance in the strip geometry is dominated by the SB resistance [10]. The SB can also be avoided in the Corbino disk geometry. Measurements showing the same effects as in Figs. 1 to 5 will be presented elsewhere [11].

We now analyze the results in more detail. In Fig. 1 the resistance values have been normalized to the normal state resistance for clarity. At  $T = 95\text{K}$  the resistances are 0.23 and 0.62  $\Omega$  before and after cutting, respectively. Below  $T_c$ , however, the effect of the SB on reducing the resistance of the strip crystal is very pronounced. The maximum relative change in the resistance is observed at fields of the order of 500 Oe, decreases gradually at higher fields, and tends to become negligible at fields of about 2T. Such a decrease of the SB with increasing field is expected theoretically [5]. Another important observation is that the relative change in the resistance generally grows with decreasing temperature. At low temperatures the resistance is commonly expected to be governed by bulk pinning, which should dominate over the SB. However, this is just contrary to the behavior observed in Fig. 1: Thermal activation over the SB, which decreases with decreasing temperature, remains the dominant limitation

for vortex motion in the strip samples, and even becomes more important, as the temperature is decreased. In other words, whenever vortex flow is large enough for a finite resistance to be detected, the corresponding measured resistance in the strip geometry is governed by the SB rather than the bulk properties, except close to  $T_c$  or at high fields.

In addition to altering the value of the resistance, the SB also governs the measured activation energy. Figure 2 shows the effective activation energy  $U$  as obtained by a linear fit to the Arrhenius data of Fig. 1 (for fields below 1000 Oe the Arrhenius part in the vortex-liquid phase above the melting kink is used). The activation energy of the strip is significantly larger than that of the square crystal indicating that  $U$  of the SB is significantly larger than the vortex pinning  $U$  in the bulk. Since in both geometries the bulk and surface contributions are partially intermixed, we believe that the strip values of  $U$  reflect a lower bound for the SB activation energy, whereas the square sample  $U$  is the upper bound for the bulk activation. The activation energies of our strip samples are comparable to the values reported in the literature [12,13].

The SB also dominates the nonlinear characteristics of the resistive behavior. Figure 3 shows the normalized  $R(T)$  of crystal B at 700 Oe for various currents. The square crystal, governed by the bulk properties, displays nearly linear resistance, except at the lowest temperature, as shown for the 5 and 15 mA current (thick curves). The SB dominated strip crystal, in contrast, shows highly nonlinear resistance at low currents, as seen in Fig. 3, which tends to approach the bulk value as the current is increased. At low currents the transmissivity of the SB is low and thus the resistance of the strip crystal is significantly reduced. The height of the SB decreases with increasing transport current, resulting in a nonlinear resistance [6]. This fundamental property of the SB is the main source of the apparent nonlinear resistive behavior in the vortex-liquid phase, which was previously ascribed to a liquid state with high bulk viscosity [14].

We now focus on the resistive kink at the first-order vortex lattice phase transition (FOT) [15,16]. Upon freezing, the resistance in BSCCO crystals is observed to drop sharply below the noise level [17,18]. This behavior is often ascribed to the sudden onset of bulk pinning. We now proceed to evaluate the contribution of the SB to this resistive transition. Figure 4(a) shows  $R(T)$  of crystal B at 300 Oe in the vicinity of the FOT at a relatively high current of 10mA in order to resolve the behavior in the solid phase. The square crystal reflects the behavior of the bulk resistance  $R_B$  which shows an appreciable drop upon freezing. However, the important observation here is that the strip sample exhibits an even larger drop and a significantly lower resistance in the solid phase. This means that in the strip samples the SB dominates the resistive behavior also in the solid phase.

Figure 4(b) shows the ratio of the normalized resistances  $R_{square}/R_{strip}$  which reflects the ratio  $R_B/R_S$ . In the fluid the edge resistance  $R_S$  is lower than  $R_B$  resulting in a ratio  $R_{square}/R_{strip} > 1$ . However, upon freezing,  $R_S$  drops dramatically resulting in as much as two orders of magnitude increase in  $R_{square}/R_{strip}$  in Fig 4(b). This result demonstrates that the SB itself undergoes a sharp transition from a relatively low barrier height in the fluid phase to significantly enhanced barrier in the solid phase. Such a transition is indeed expected theoretically for the melting (vortex solid to line liquid) and, even more so, for the sublimation (vortex solid to pancake gas) transition [6,19]. In the pancake gas the vortex penetration is accomplished by activation of individual pancakes, which is a relatively easy process. In the solid phase, on the other hand, an extended line vortex has to penetrate and to distort the solid lattice in the bulk, which results in large activation energy [19]. Figure 4 is therefore a direct manifestation of the sharp transition of the SB that occurs concurrently with the bulk FOT. This finding is consistent with the conclusions from the self-field studies [3]. Upon freezing both  $R_B$  and  $R_S$  drop sharply. However, since  $R_S$  dominates the resistance both above and below the FOT, it is important to realize that the resistive transition that is usually measured in strip-shaped BSCCO crystals mainly reflects the sharp drop of  $R_S$ , rather than of  $R_B$  which is obscured by the SB.

The particularly large SB in the vortex-solid phase results usually in immeasurably low resistance below the FOT. The use of the square crystals provides therefore a unique method to study the true bulk vortex properties in the quasi-lattice or Bragg glass phase [20–23] below the FOT. Figure 5 shows an example of the resistive behavior of square crystal at 100 Oe for various currents. In contrast to the strip crystal for which the apparent resistance drops rapidly to below the noise level (dashed curve), the bulk resistance of the square sample can be measured down to as much as 20 K below the FOT at elevated current. In addition, in contrast to the vortex-fluid phase, which shows almost linear behavior above the FOT, the quasi-lattice displays a highly nonlinear resistivity. The bulk resistance is thermally activated with activation energy being strongly current dependent. The inset to Fig. 5 shows the values of  $U$  obtained by a linear fit to the Arrhenius data for 100, 300, and 500 Oe. The activation energy has approximately power-law dependence,  $U \propto I^{-\mu}$ , with  $\mu \approx 0.5$ . This power-law current dependence in the vortex-solid is expected from recent theoretical treatments of the Bragg glass phase [1,20–23]. Furthermore, the same theories predict a weak field dependence of  $U$ , also in agreement with the inset to Fig. 5. These results, without the influence of the SB, provide therefore a first experimental test of the Bragg glass theories by transport measurements in BSCCO.

In summary, we have demonstrated that in the conventional strip geometry the SB dominates the resistive

behavior of BSCCO crystals over a wide range of temperatures and fields. The SB governs the value of the resistance, its nonlinear behavior, the apparent activation energy, and the resistance drop at the first-order transition. The true bulk properties can be probed using an alternative configuration in which the electrical contacts are well separated from the edges of large crystals. This geometry provides an important new access for investigation of the transport properties in the Bragg glass phase below the FOT.

Helpful discussions with V. B. Geshkenbein, T. Giamarchi, P. Le Doussal, T. Nattermann and J. Kierfeld are gratefully acknowledged. This work was supported by the Israel Ministry of Science and the Grant-in-Aid for Scientific Research from the Ministry of Education, Science, Sports and Culture, Japan, by the Israel Science Foundation, and by the MINERVA Foundation, Munich, Germany.

- 
- [1] G. Blatter *et al.*, Rev. Mod. Phys. **66**, 1125 (1994); E. H. Brandt, Rep. Prog. Phys. **58**, 1465 (1995).
  - [2] D. T. Fuchs *et al.*, Nature **391**, 373 (1998).
  - [3] D. T. Fuchs *et al.*, Phys. Rev. Lett. **80**, 4971 (1998).
  - [4] C. P. Bean and J. D. Livingston, Phys. Rev. Lett. **12**, 14 (1964).
  - [5] J. R. Clem, Low Temp. Physics - LT 13, Vol. 3, eds. K.D. Timmerhaus *et al.* (Plenum, New York, 1974) p. 102.
  - [6] L. Burlachkov, A. E. Koshelev, and V. M. Vinokur, Phys. Rev. B **54**, 6750 (1996).
  - [7] M. Benkraouda and J. R. Clem, unpublished.
  - [8] N. Motohira *et al.*, J. Ceram. Soc. Jpn. **97**, 994 (1989).
  - [9] B. Khaykovich *et al.*, Phys. Rev. Lett. **76**, 2555 (1996).
  - [10] D. T. Fuchs and E. Zeldov, unpublished.
  - [11] R. A. Doyle *et al.*, unpublished.
  - [12] T. T. M. Palstra *et al.*, Phys. Rev. Lett. **61**, 1662 (1988).
  - [13] R. Busch *et al.*, Phys. Rev. Lett. **69**, 522 (1992).
  - [14] T. Tsuboi, T. Hanaguri, and A. Maeda, Phys. Rev. B **55**, 8709 (1997).
  - [15] H. Safar *et al.*, Phys. Rev. Lett. **69**, 824 (1992).
  - [16] W. K. Kwok *et al.*, Phys. Rev. Lett. **69**, 3370 (1992).
  - [17] D. T. Fuchs *et al.*, Phys. Rev. B **54**, 796 (1996); S. Watauchi *et al.*, Physica C **259**, 373 (1996).
  - [18] D. T. Fuchs *et al.*, Phys. Rev. B **55**, R6156 (1997).
  - [19] A. E. Koshelev, Physica C **223**, 276 (1994).
  - [20] T. Nattermann, Phys. Rev. Lett. **64**, 2454 (1990).
  - [21] T. Giamarchi and P. Le Doussal, Phys. Rev. Lett. **72**, 1530 (1994); Phys. Rev. B **52**, 1242 (1995).
  - [22] J. Kierfeld, Physica C **300**, 171 (1998); J. Kierfeld, T. Nattermann and T. Hwa, Phys. Rev. B **55**, 626 (1997).
  - [23] D. Ertas and D. R. Nelson, Physica C **272**, 79 (1996); V. M. Vinokur *et al.*, Physica C **295**, 209 (1998).

## FIGURE CAPTIONS

Fig. 1. Arrhenius plot of the normalized resistance of BSCCO crystal A in the square geometry (thick curves), and after cutting into a strip (thin curves), for various applied fields between 92 and 5000 Oe ( $I = 1$  mA). Inset: Schematic sample geometry. Four probe resistance was measured on a square crystal (thick perimeter) with contacts deposited in the center. The crystal was then cut into a strip along the marked lines (thin lines) and remeasured.

Fig. 2. The activation energy  $U$  as a function of applied field for the square ( $\square$ ) and strip ( $\circ$ ) sample geometries. The activation energies were obtained by a linear fit to the Arrhenius part in the vortex-liquid phase of Fig. 1.

Fig. 3. Arrhenius plot of the normalized resistance

of crystal B at 700 Oe. Thick curves: resistance of the square sample at 5 and 15 mA current. Thin curves: nonlinear resistance in the cut strip geometry for 0.5 to 15 mA currents.

Fig. 4. (a) Normalized  $R(T)$  of the square and strip crystal B in the vicinity of the FOT at 300 Oe and 10 mA current. (b) The ratio of the normalized square and strip resistances from (a).

Fig. 5. Arrhenius plot of the normalized resistance of the square sample B at 100 Oe and various currents between 1 and 30 mA. The dashed curve is the normalized resistance of the strip at 3 mA for comparison. Inset: Activation energy as a function of current in the vortex-solid phase at applied fields of 100 Oe ( $\bullet$ ), 300 Oe ( $\times$ ), and 500 Oe ( $\square$ ). Solid line:  $U = CI^{-0.5}$  with  $C=5200$  K mA<sup>0.5</sup>.

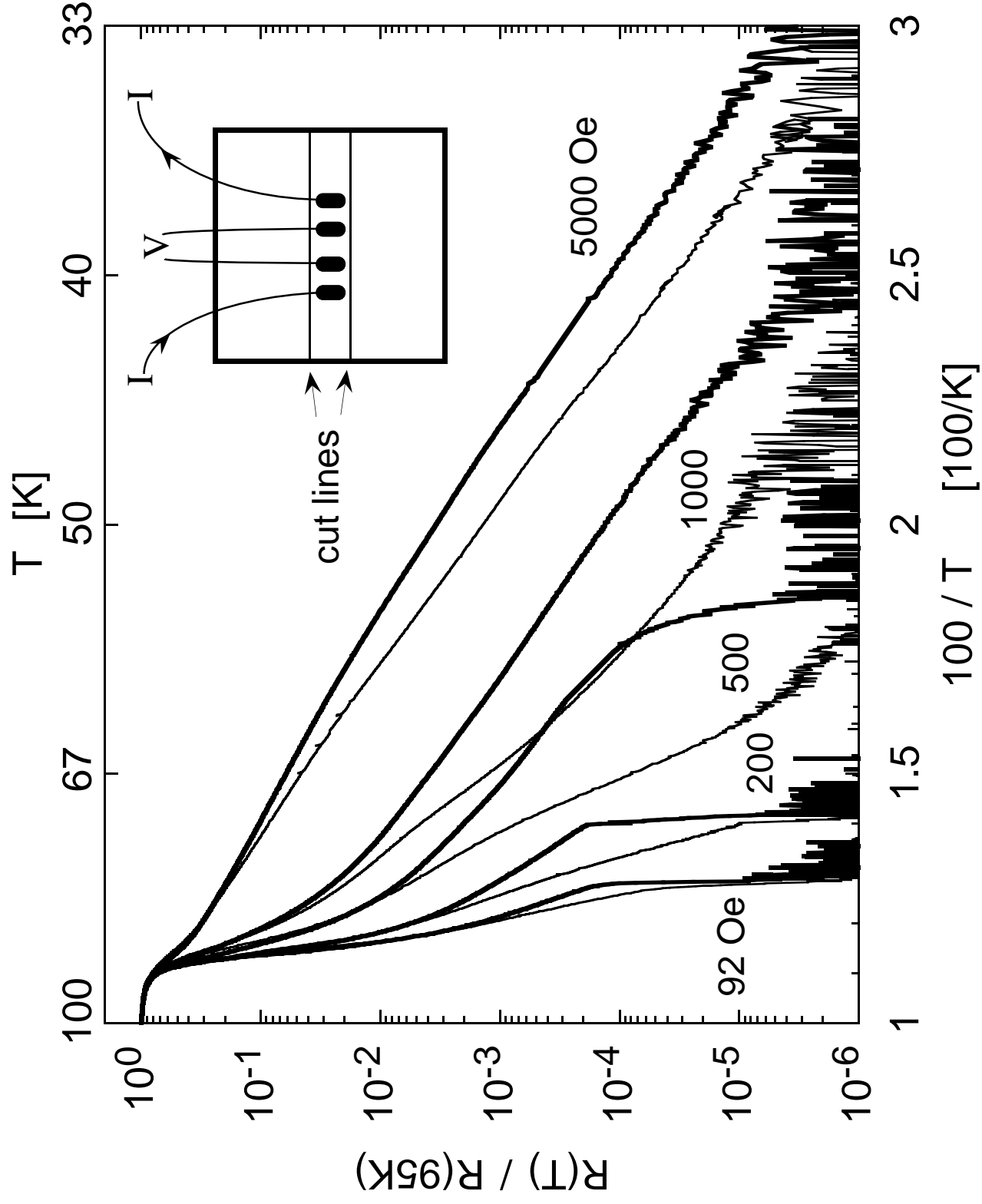


Figure 1, Fuchs et al.

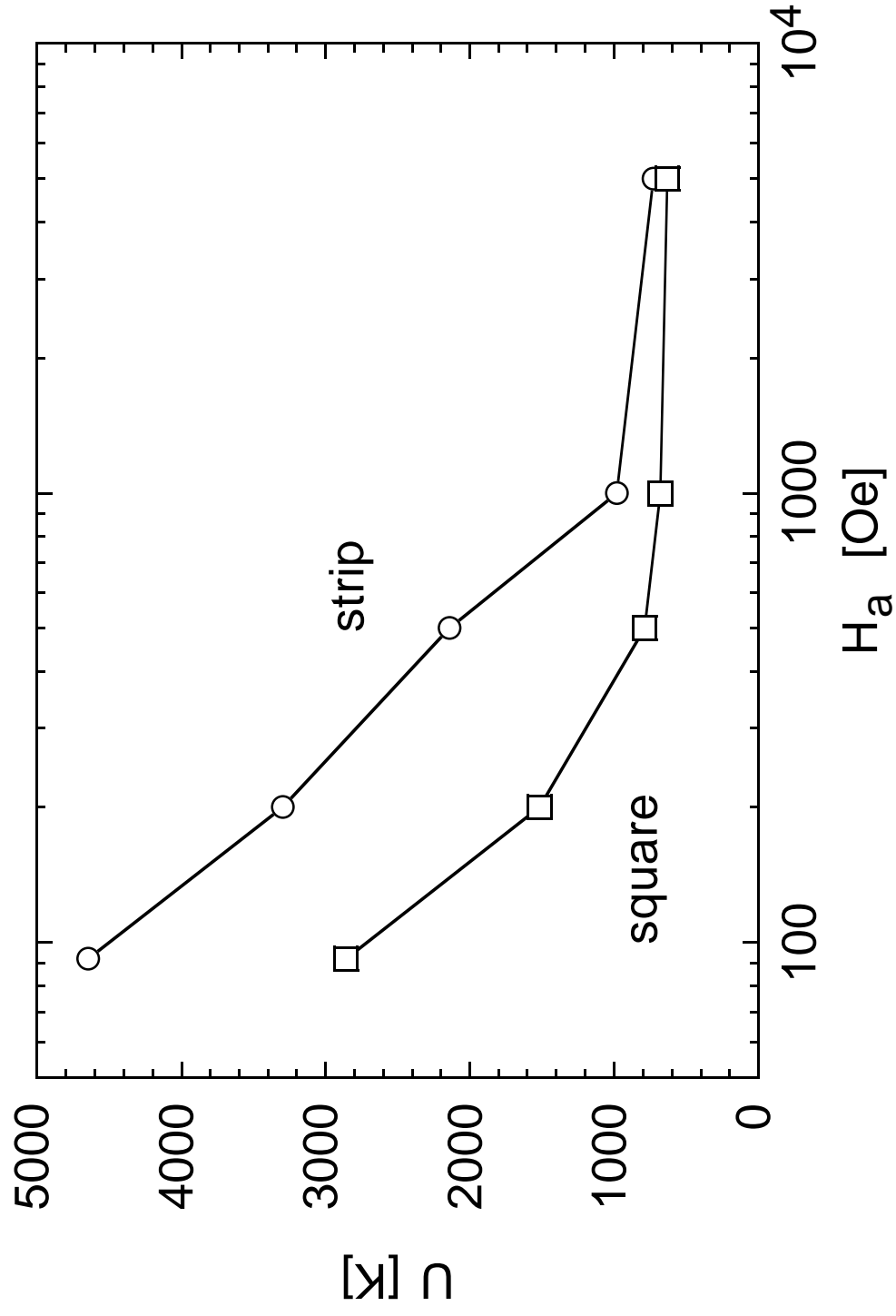


Figure 2, Fuchs et al.

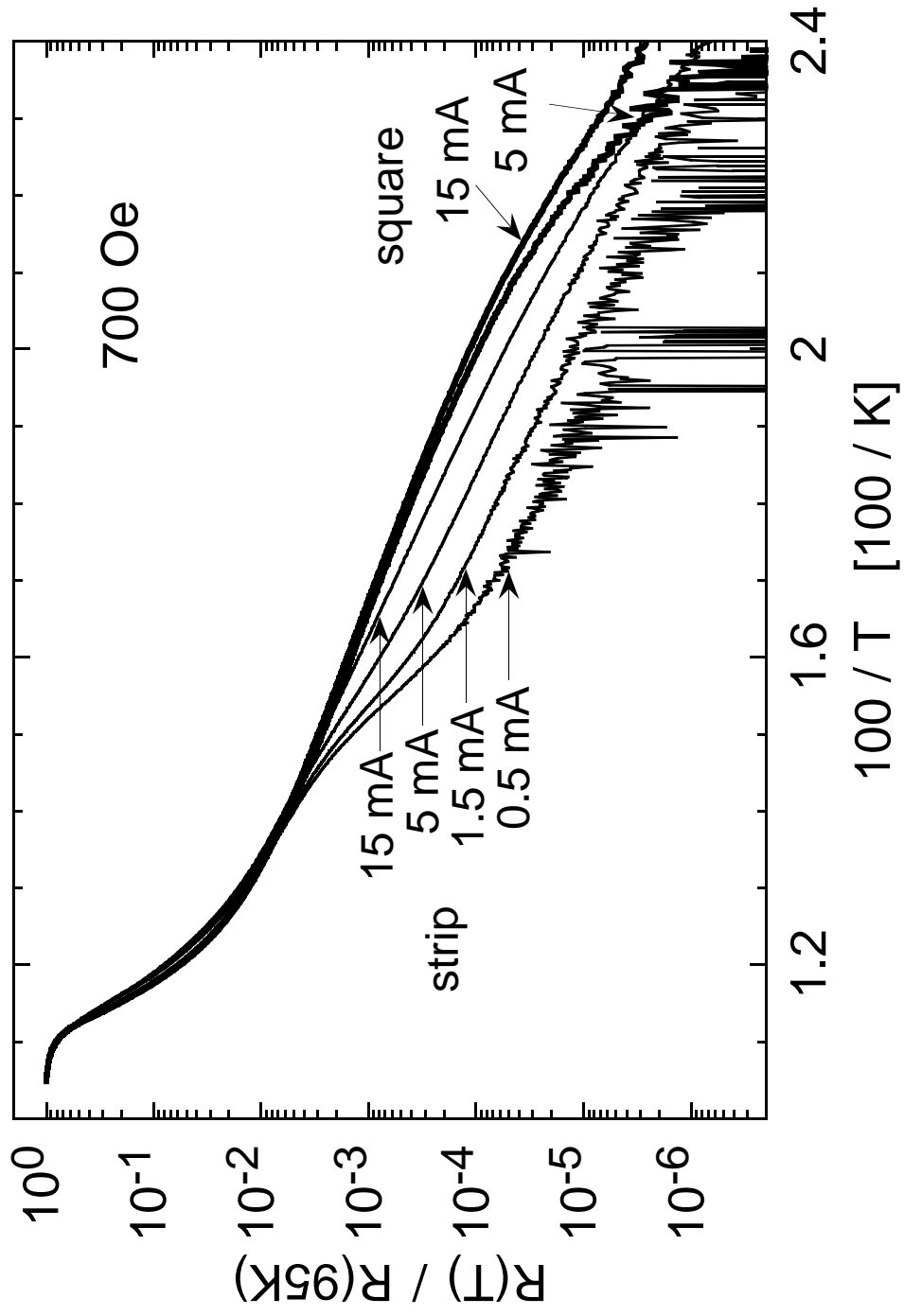


Figure 3, Fuchs et al.

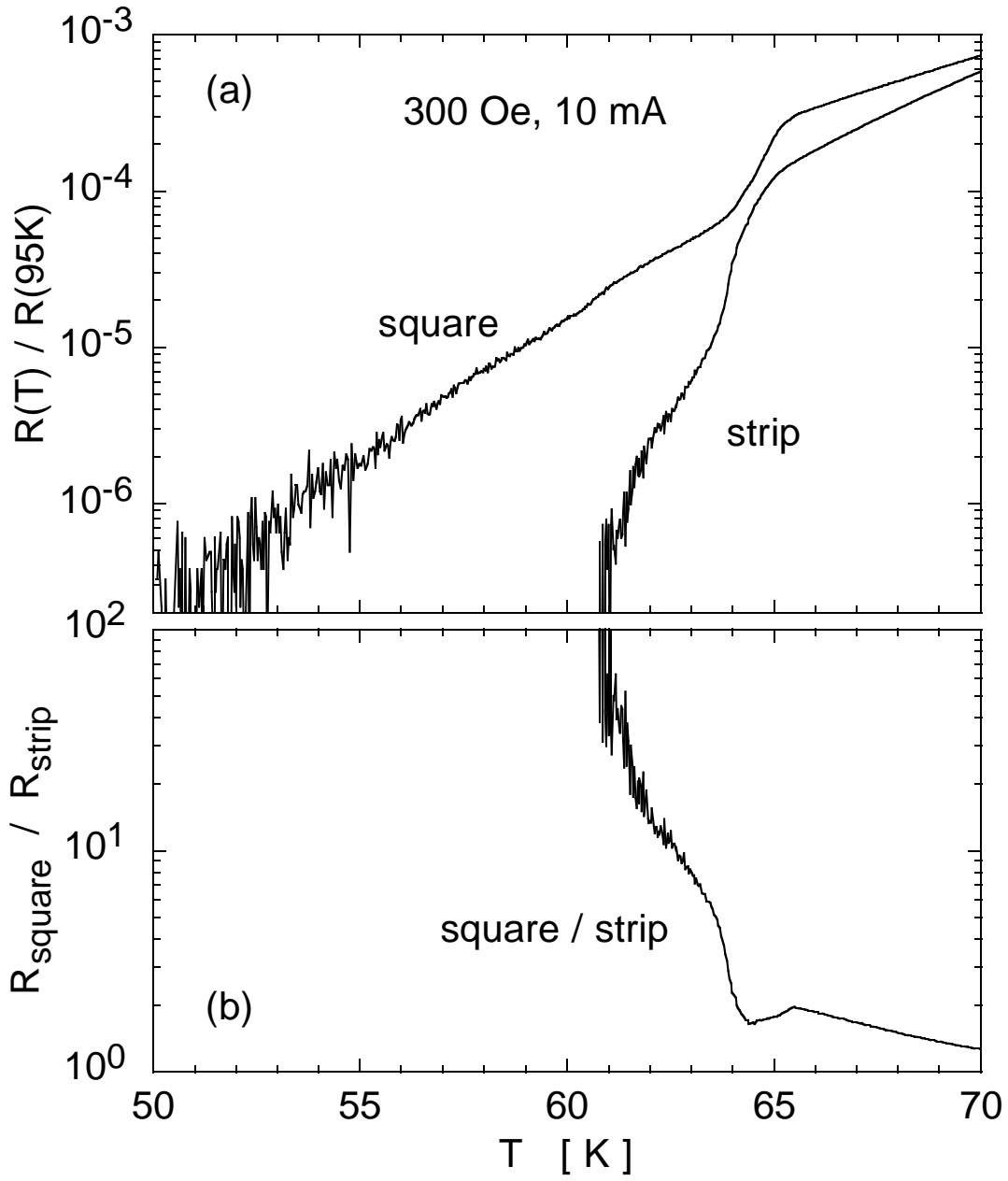


Figure 4, Fuchs et al.

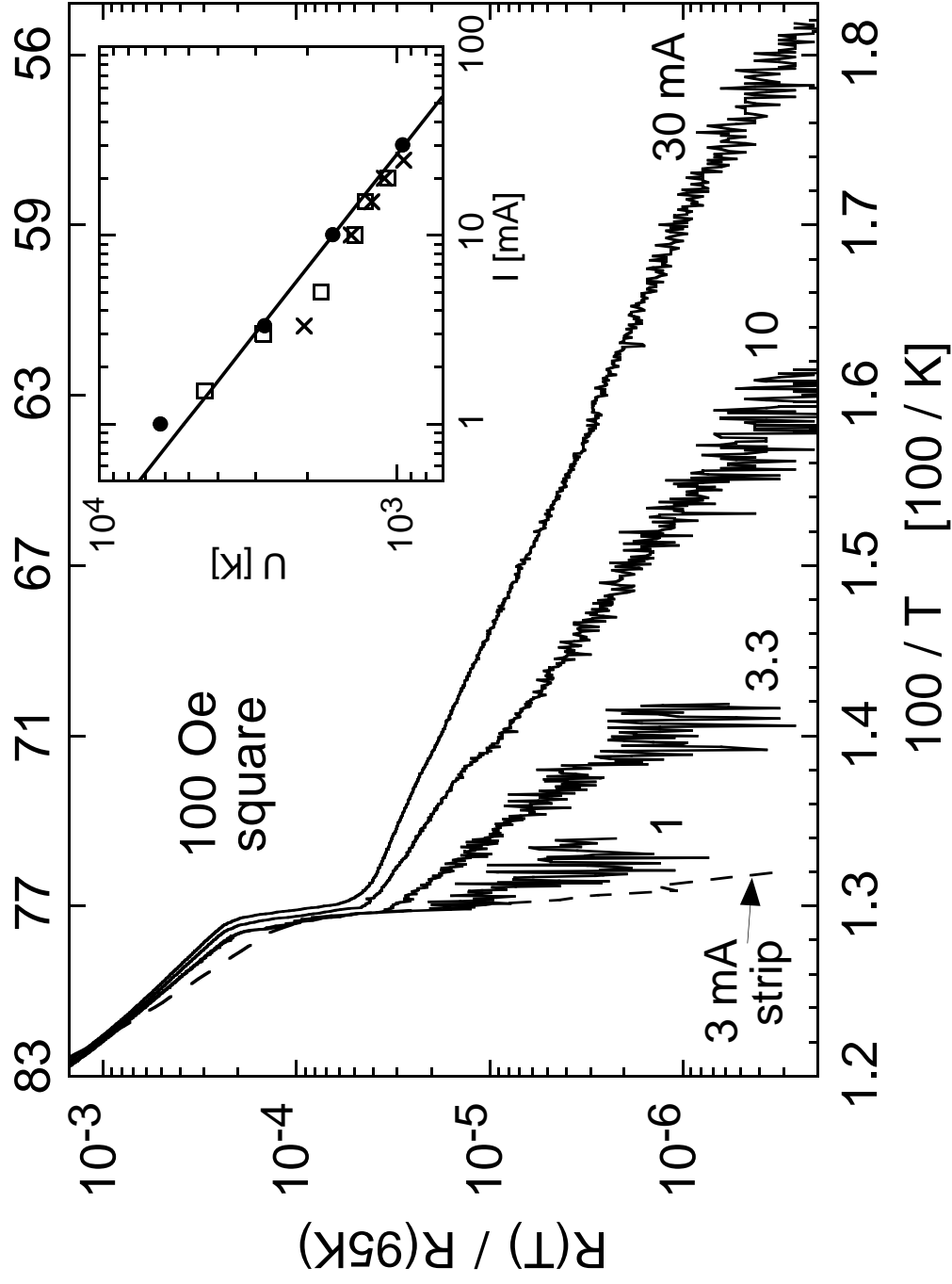


Figure 5, Fuchs et al.